Multidisciplinary Studies Exploring Extreme Proterozoic Environment Conditions, AGU Geophysical Monograph

Analysis of Carbon Cycle System during the Neoproterozoic: Implication for Snowball Earth Events

Eiichi Tajika

Department of Earth and Planetary Science, University of Tokyo, Tokyo, Japan.

Carbon cycle and climate change during the Neoproterozoic have not been understood well. In that period, global glaciations may have occurred several times. Carbon isotopic composition of seawater was generally heavy and fluctuated with very large amplitudes, suggesting unusual behaviors of the carbon cycle system. In this study, the carbon cycle and the climate change during the Neoproterozoic are analyzed quantitatively using an improved carbon isotope mass balance model with a one-dimensional energy balance climate model. According to the results, the organic carbon burial rate is generally high and the carbonate precipitation rate is generally low through the Neoproterozoic. However, before the glaciations, the organic carbon burial increases and the carbonate precipitation decreases. On the other hand, the organic carbon burial decreases and the carbonate precipitation increases after the glaciations. Because the carbonate precipitation rate should balance with the cation supply rate due to chemical weathering, the climate factors (i.e., T and pCO_2) also decrease before the glaciations and increase after the glaciations. The climate is, however, too warm to initiate glaciations when present values of the CO_2 degassing rate and the organic carbon weathering rate are assumed in the model. If the global glaciations were caused at the positive excursions of $\delta^{13}C$, the CO_2 degassing rate should have decreased to < 1/4-1/2 times the present rate at the same time. In order to reconstruct the carbon cycle and the climate change in further detail, we need to know variations of the tectonic forcing (e.g., volcanic activities) during the Neoproterozoic.

1. INTRODUCTION

Climate change during the Proterozoic seems to be enigmatic. There are ice ages in the Early Proterozoic (the Huronian glaciations) and in the Late Proterozoic (the Sturtian and the Varanger-Marinoan glaciations) [e.g., *Hambrey and Harland*, 1981; *Crowell*, 1999]. Each episodes may have multiple glacial events (at least, more than a single event) suggested from existence of multiple diamictite layers and carbon isotopic excursions, although the exact number of glacial events has been controversial [e.g., *Kaufman et al.*, 1997; *Kennedy et al*, 1998; *Hoffman and Schrag*, 2002]. On the other hand, although possible glacial deposits have been found in north-central Siberia and north Scotland [e.g., *Crowell*, 1999], there is no certain evidence of glaciations during the Middle Proterozoic. Therefore, two big ice ages are separated by a 1.5-billion-year warm period during the Proterozoic.

Paleomagnetic studies have revealed that there is evidence for low-latitude ice sheets both in the Late and the Early Proterozoic glaciations [e.g., *Evans*, 2000]. There are also several features associated with the Proterozoic glaciations. Glacial diamictites in the Neoproterozoic are overlain by thick carbonate sediments (called “cap carbonate”) which may have deposited under tropical environment, showing unusual textures and low values of carbon isotopic composition [*Hoffman et al*., 1998a, b; *Hoffman and Schrag*, 2002]. There are iron formation and manganese deposit associated with the glaciogenic deposits [*Kirschvink*, 1992; *Kirschvink et al*., 2000]. In order to interpret these features peculiar to the Proterozoic glaciations, *Kirschvink* [1992] has proposed the snowball Earth hypothesis,

that is, most of the Earth's surface may have been globally ice-covered during the Proterozoic ice ages. Although there are several arguments for this hypothesis (equatorial surface oceans may not have been frozen completely, etc.) [e.g., *Hyde et al.*, 2000; *Poulsen et al.*, 2001] or there is another interpretation of low-latitude ice-sheets (obliquity of the Earth may have been very large before the end of Precambrian) [e.g., *Williams*, 1993; *Jenkins*, 2000], this might be the only hypothesis which can explain all of the unusual features associated with glaciogenic deposits described above [*Kirschvink*, 1992, 2002; *Hoffman et al*., 1998b; *Hoffman and Schrag*, 2002]. Because the susceptibility of the Earth to global glaciations during the Proterozoic would have been similar to that of today in spite of dimmer Sun earlier in Earth's history [*Tajika*, 2003], we need to study behaviors of carbon cycle during the Proterozoic.

Carbon isotopic composition of seawater recorded in sedimentary rocks may provide useful information on variation of carbon cycle and climate change. Carbon isotopic composition (the $\delta^{13}C$ value) during the Neoproterozoic is generally heavier than that during the Phanerozoic, and shows variations with very large amplitudes (Figure 1) [e.g., *Kaufman et al.*, 1997; *Hayes et al.*, 1999]. These features should be the results of variations of the carbon cycle system, such as variations of organic carbon burial rate. The oscillations of carbon isotopic composition may closely link with the global glaciations (Figure 1), and unusually high rate of organic carbon burial suggested from positive excursions of $\delta^{13}C$ may have facilitated the global glaciations by reducing atmospheric CO_2 level [e.g., *Kaufman et al*., 1997; *Hoffman et al*., 1998a, b]. Variations of the carbon cycle system and the atmospheric CO_2 levels during the Neoproterozoic, however, have not been studied quantitatively.

In this study, a carbon isotope mass balance model is improved and combined with a one-dimensional energy balance climate model in order to analyze the carbon cycle system and the climate system during the Neoproterozoic. In this model, variations of carbon fluxes due to several processes such as organic carbon burial, carbonate precipitation, and carbonate/silicate weathering can be estimated using time-series data set of carbon isotopic composition of seawater, and, then, partial pressure of CO_2 and surface temperatures can be estimated through the climate model. Implication for the global glaciations will also be discussed in the context of variations of the carbon cycle.

2. MODELS

Carbon isotope mass balance models have been developed and used in order to study variations of the carbon cycle system during geologic time. The model usually considers both carbon mass balance and carbon isotope mass balance with respect to the atmosphere-ocean system. The atmosphere-ocean system is assumed in a steady state because the model is usually applied to the problem on long timescale (longer than the residence time of carbon in the atmosphere-ocean system, i.e., $> 10^5$ years), although the carbon isotope record during the Neoproterozoic might be better understood with the nonsteady dynamics of two reactive pools of carbon in the oceans [*Rothman et al*., 2003].

In the carbon isotope mass balance model, riverine input of carbon into the atmosphere-ocean system (F_r) with the $\delta^{13}C$ value of the total sedimentary carbon ($\delta^{13}C_r$) should balance with output of carbon due to carbonate precipitation (F_B^C) with the $\delta^{13}C$ value of seawater ($\delta^{13}C_a$) and organic carbon burial (F_B^O) with the $\delta^{13}C$ value of organic carbon ($\delta^{13}C_g$). Therefore, mass balance equations are represented by

$$F_r = F_B^C + F_B^O \tag{1}$$

$$\delta^{13}C_r F_r = \delta^{13}C_a F_B^C + (\delta^{13}C_a - \Delta) F_B^O \tag{2}$$

where Δ represents a net difference of $\delta^{13}C$ values between inorganic carbon and organic carbon ($= \delta^{13}C_a - \delta^{13}C_g$), which actually includes effect of carbon isotopic fractionation due to photosynthesis, isotopic difference between dissolved CO_2 and dissolved inorganic carbon, isotopic difference between dissolved inorganic carbon and carbonate minerals, and isotopic shift associated with secondary biological processes [e.g., *Hayes et al.*, 1999]. When there is time-series data set of $\delta^{13}C_a$ with assumed values of $\delta^{13}C_r$ and Δ, the factor f_o which represents the fraction of carbon that is buried in organic form can be obtained.

$$f_o = F_B^O/(F_B^C + F_B^O) = (\delta^{13}C_a - \delta^{13}C_r) / \Delta. \tag{3}$$

This is essential information obtained from the carbon isotope mass balance model. Here, if we assume the riverine flux of carbon F_r in addition to $\delta^{13}C_r$ and Δ, two unknown fluxes (F_B^C and F_B^O) can be estimated separately from the equations (1) and (2) as follows:

$$F_B^C = (\Delta - \delta^{13}C_a + \delta^{13}C_r) F_r / \Delta \tag{4}$$

$$F_B^O = (\delta^{13}C_a - \delta^{13}C_r) F_r / \Delta. \tag{5}$$

To summarize, using the two equations of (1) and (2), we can estimate two unknown parameters (F_B^O and F_B^C) when other parameters (F_r, $\delta^{13}C_r$, and Δ) are assumed to be constant, and time-series data set of $\delta^{13}C_a$ is given as input data.

Next, we improve this simple model to include weathering fluxes and degassing flux in order to discuss climate changes and roles of each carbon flux in the carbon cycle system. The carbon flux into the atmosphere-ocean system is divided into three fluxes, that is, degassing of CO_2 via metamorphism and volcanism (F_D), weathering of carbonate (F_W^C), and oxidative weathering of organic carbon (F_W^O). Each carbon source has each specific carbon isotope value (represented here as $\delta^{13}C_M$, $\delta^{13}C_C$, and $\delta^{13}C_O$, respectively). In this case, the carbon mass balance and the carbon isotope mass balance equations are represented by

$$F_D + F_W^C + F_W^O = F_B^C + F_B^O \quad (6)$$

$$\delta^{13}C_M F_D + \delta^{13}C_C F_W^C + \delta^{13}C_O F_W^O = \delta^{13}C_a F_B^C + (\delta^{13}C_a - \Delta) F_B^O. \quad (7)$$

In order to solve these equations, we need additional constraints and assumptions. One is the alkalinity budget in the ocean, that is,

$$F_B^C = F_W^C + F_W^S \quad (8)$$

where F_W^S represents silicate weathering rate. This equation represents a net carbonate precipitation (difference between the rates of the precipitation and the weathering of carbonates) which should be equal to the cation supply derived from the chemical weathering of silicate minerals [*Berner*, 1991, 1994].

Because Δ varies with concentration of dissolved CO_2 (hence partial pressure of atmospheric CO_2, that is, pCO_2) as well as other factors such as growth rate and the ratio of cellular volume to surface area of phytoplankton [e.g., *Bidigare et al.*, 1997; *Kump and Arthur*, 1999], and also because pCO_2 must have changed greatly through the ice ages, variations of Δ should be important during the Neoproterozoic.

Hayes et al. [1999] compiled not only $\delta^{13}C_a$ data but also $\delta^{13}C_g$ data to estimate variations of Δ during the later Neoproterozoic (between 800 Ma and 540 Ma). The method they adopted is: (1) samples were sorted in order of assigned age, thus producing a sequence in which samples from different tectonic provinces were interspersed, and (2) values of $\delta^{13}C_a$ and $\delta^{13}C_g$ were compared among samples with closely similar ages, without regard for location [*Hayes et al*., 1999]. Therefore, validity of the approach depends on the accuracy of the age assignments that guide the comparisons [*Hayes et al*., 1999]. Although this method may be the best way to compile existing data sets to compare among samples from different localities, uncertainties due to age assignments cannot be eliminated. Therefore, although we use the data sets of $\delta^{13}C_a$ and $\delta^{13}C_g$ compiled by *Hayes et al.* [1999], we also use higher resolution data set of $\delta^{13}C_a$ compiled also by *Hayes et al*. [1999] (Figure 1) and the theoretical formulation of Δ proposed by *Kump and Arthur* [1999]. The formulation of Δ as a function of pCO_2 is expressed as

$$\Delta = A/(B \times pCO_2) - 33 \quad (9)$$

where A=2301.91 and B=0.034 [*Kump and Arthur*, 1999]. This formulation is based on data set for haptophyte algae [*Bidigare et al.*, 1997] with Henry's Law at 25°C and $[PO_4]$ = 0.25 μmol/kg. Although this may not be appropriate for the Neoproterozoic ocean and biosphere, we will use this formulation as one of possible expressions of Δ as a function of pCO_2.

The chemical weathering reaction is known to have dependencies on temperature (T) and pCO_2 [e.g., *Walker et al.*, 1981; *Schwartzman and Volk*, 1989, 1991; *Berner*, 1991, 1994]. A function f_B which represents the dependencies of weathering rate on T and pCO_2 is assumed here as follows [e.g., *Walker et al.*, 1981; *Schwartzman and Volk*, 1989, 1991; *Tajika and Matsui*, 1990, 1992; *Tajika*, 2003]:

$$f_B = (pCO_2/pCO_2^*)^n \exp(-E/RT) \quad (10)$$

where n is an exponent of pCO_2 dependency, E is activation energy of reaction, R is gas constant, and * represents the present value. For Ca-, Mg-silicates exposed on the continents of an abiotic Earth, n is probably between 0.3 and 0.4 [*Schwartzman and Volk*, 1989]. For simplicity, we assume 0.3 [*Walker et al*., 1981; *Schwartzman and Volk*, 1989, 1991; *Tajika and Matsui*, 1990, 1992] in this study. Activation energy of chemical dissolution of various silicates is estimated ranging from 10 to 20 kcal/mol [*Schwartzman and Volk*, 1989; *Lasaga et al*., 1994]. We use 15 kcal/mol [*Berner*, 1994] in this study. For simplicity, a dependency of the weathering rate on temperature through runoff is not considered (hence negative feedback should be minimum strength). Similarly, other factors (such as river runoff due to changes in paleogeography, land area, uplift and physical erosion, and lithology) are not considered here for simplicity. The silicate and carbonate weathering rates are assumed here as

follows:

$$F_W^S = f_B(T, pCO_2)\, f_E\, F_W^{S*} \quad (11)$$

$$F_W^C = f_B(T, pCO_2)\, f_E\, F_W^{C*} \quad (12)$$

where f_E is a soil biological activity factor which represents efficiency of weathering due to plants and microbes on land [*Schwartzman and Volk*, 1989, 1991; *Berner*, 1991, 1994].

Plants accelerate the uptake of CO_2 during weathering by secretion of organic acids by roots and associate symbiotic microflora, recirculation of water by transpiration and accelerated rainfall, and retention by roots of soil from removal by erosion [*Schwartzman and Volk*, 1989, 1991; *Berner*, 1991, 1994]. Because there were not higher terrestrial plants before the Silurian, efficiency of silicate weathering rate due to the soil biological activity should have been very low during the Neoproterozoic ($f_E << 1$) compared to that at present ($f_E = 1$). However, microbial and possibly lichen colonization on the continents in the Precambrian probably resulted in a considerable increase in chemical weathering relative to abiotic conditions [*Schwartzman and Volk*, 1989]. The factor before the Silurian may be estimated from the weathering rate in unvegetated region on the present Earth. On the basis of such an estimate [*Drever and Zobrist*, 1992], a value for f_E of 0.15 [*Berner*, 1994] is assumed in this study.

We combine the carbon isotope model described above with a simple climate model. We use a one-dimensional energy balance climate model (1D-EBM) with CO_2-dependent outgoing radiation [*Caldeira and Kasting*, 1993; *Ikeda and Tajika*, 1999]. The model is based on the Budyko-Sellers-type EBM, which employs diffusive-type of heat transport and discontinuous albedo at the ice cap edge, and takes into account dependency of CO_2 on the outgoing infrared radiation (see *Caldeira and Kasting* [1993] and *Ikeda and Tajika* [1999]). From this model, we can estimate latitudinal temperature distribution as functions of the effective solar constant (S_{eff}) and pCO_2.

Figure 2a shows an example of variations of latitudinal temperature distribution (S_{eff} is assumed to be 0.94 for the Neoproterozoic). As pCO_2 decreases, temperature lowers at every latitude, although the tropics remains warmer. However, when pCO_2 achieves the critical level at which the stable solution for partially ice-covered branch disappears, the Earth becomes globally ice-covered (under freezing condition globally). The critical level of pCO_2 depends on model parameters (albedo and diffusion coefficient) and also on climate models (EBMs, Atmospheric GCMs, or Atmosphere-Ocean-Coupled-GCMs), but the basic behaviors of the climate system, that is, global cooling due to pCO_2 decrease and globally freezing condition at very low CO_2 level, might be the same [e.g., *Jenkins and Smith*, 1999] (note, however, that there may be a quasi-stable state of ice-covered Earth with an equatorial open ocean [e.g., *Hyde et al.*, 2000]). In the following arguments, we assume this relationship as the most likely behaviors of the climate system for the case of pCO_2 decrease.

We estimate global chemical weathering rate from these temperature distributions and pCO_2 conditions. Figure 2b shows a relationship between pCO_2 and the global silicate weathering rate, which is obtained from the integration of the silicate weathering rate from the pole to the equator as a function of temperature at each latitude. For simplicity, we assume uniform distribution of continents and oceans from the pole to the equator as an ideal case. If continents concentrate in low latitudes and contribution of chemical weathering in low latitude is large, then the curve would shift rightward in this diagram (Figure 2b). The chemical weathering is assumed to occur as long as the surface temperature is above 0^oC. When we obtain the silicate weathering rate from the carbon isotope model described above, we can estimate pCO_2 and the temperature distribution (or the globally-averaged surface temperature, T_S) from this relationship.

To summarize, using the six equations of (6)-(9), (11), and (12), we can estimate six unknown parameters (F_B^O, F_B^C, F_W^C, F_W^S, f_B, and Δ) when other parameters (F_D, F_W^O, $\delta^{13}C_C$, $\delta^{13}C_O$, and $\delta^{13}C_M$) are assumed to be constant and time-series data set of $\delta^{13}C_a$ is given as input data. When we combine the carbon isotope model with the climate model, we can further estimate pCO_2 and T_S.

3. RESULTS AND DISCUSSION

As a standard case, we assume the present values of F_D (= 7.9 x 10^{12} mol/year) and F_W^O (= 3.75 x 10^{12} mol/year) [*Berner*, 1991], and average isotopic values of $\delta^{13}C_C$ (=0 ‰), $\delta^{13}C_O$ (= -25 ‰), and $\delta^{13}C_M$ (= -5 ‰) [e.g., *Schidlowski*, 1988]. We will discuss results of parameter studies in the later section. We use two kinds of data set of $\delta^{13}C_a$ for the later Neoproterozoic compiled by *Hayes et al.* [1999] as input data to the model: one is high resolution (Figure 1) and the other is low resolution but with the data set of $\delta^{13}C_g$ (i.e., with the data set of Δ).

3.1. Organic Carbon Burial

Figure 3a shows variations of the burial rate of organic carbon (F_B^O) obtained from the models. There are results for three cases: (I) high resolution $\delta^{13}C_a$ data set by *Hayes et al*. [1999] with the formulation of Δ by *Kump and Arthur* [1999] are used (solid curve), (II) low resolution $\delta^{13}C_a$ and $\delta^{13}C_g$ (i.e., Δ) data sets by *Hayes et al*. [1999] are used (dashed curve), and (III) the simple carbon isotope mass balance model (the equations (1) and (2)) with low resolution $\delta^{13}C_a$ and $\delta^{13}C_g$ (i.e., Δ) data sets by *Hayes et al*. [1999] are used (dotted curve).

As shown in this figure, the results of the Cases II and III are similar to each other. This is because the carbon isotope model depends strongly on input data of $\delta^{13}C_a$. The difference between the Cases II and III is owing to difference between the models: the model developed here (Cases I and II) may partially include the effects of climate change through variations of chemical weathering, which may affect the estimate of F_B^O. The value of F_B^O is generally high between the glaciations (especially before the glaciations), but decreases rapidly after the glaciations for all three cases. In particular, for the Case I, F_B^O becomes almost zero after the Sturtian and the Marinoan glaciations. This might be consistent with the arguments by *Hoffman et al*. [1998b]. On the other hand, before the glaciations, F_B^O becomes very high (up to 8.0-9.5 x 10^{12} mol/year) compared with the present value of 5 x 10^{12} mol/year or the values estimated for the Phanerozoic (except for the time of the Late Paleozoic glaciations) [*Berner*, 1991]. This is consistent with the view obtained from the equation (3), that is, the fraction of organic carbon burial f_o is generally higher in the Neoproterozoic than the Phanerozoic [e.g., *Hayes et al*., 1999].

It is, however, noted that absolute values of F_B^O should depend on assumed values of model parameters (especially on F_D and F_W^O, that is, the input fluxes of carbon into the atmosphere-ocean system). If these fluxes are smaller than the present values assumed here, the absolute values of F_B^O during the Neoproterozoic can be similar to or even lower than those during the Phanerozoic (see the section 3.4).

3.2. Carbonate Precipitation

Figure 3b shows variations of the carbonate precipitation rate (F_B^C) for the three cases. The carbonate precipitation rate is generally low between the glaciations (especially before the glaciations), and increases rapidly after the glaciations (part of these increases might represent precipitation of cap carbonates deposited above the glacial diamictites).

For the carbonate precipitation, the results of the Cases I and II are more similar than the result of the Case III: the amplitudes of variations are larger in the Cases I and II than in the Case III. This is because F_B^C should balance with the rate of cation supply to the ocean due to silicate and carbonate weathering, both of which depend on the climate (i.e., T and pCO_2). Because of this, the amplitudes of variations of F_B^C are larger in the model developed here (which may include the effects of climate change through the chemical weathering) than the simple carbon isotope model (which assumes constant riverine input rate).

It is, however, noted that climate change through variations of pCO_2 should be contributed not only by variations of biological forcing such as organic carbon budget and the soil biological activity, but also contributed by variations of tectonic forcing such as volcanic activity (seafloor spreading and superplume) and orogenic activity, which are not considered in the carbon isotope mass balance models. As a result, estimates of F_B^C from the carbon isotope mass balance models can only represent the contribution of variations of biological forcing.

Tajika [1999] compared the results of F_B^O and F_B^C between a simple carbon isotope mass balance model and a "full" model of the carbon cycle (similar to GEOCARB model developed by *Berner* [1994]). According to the result, the estimates of F_B^O from the two models seem to be very similar to each other except for their absolute values. On the other hand, the estimates of F_B^C from the two models are quite different. The result of the simple model clearly reflects the input data of $\delta^{13}C$. Because riverine inputs of carbon and calcium to the ocean due to chemical weathering must depend largely on T and pCO_2 (which should be affected both by the biological forcing and the tectonic forcing), both the pattern and the absolute values of F_B^C are different between the results of the two different methods.

Therefore, it appears that the simple carbon isotope mass balance models would be useful for estimating the pattern of F_B^O, but may not be appropriate for its absolute value, and cannot estimate F_B^C [*Tajika*, 1999]. Because the model developed in this study may include effects of climate change through the chemical weathering, the amplitudes of variations of carbon fluxes (including F_B^O and F_B^C) would be estimated more properly than those estimated from the simple carbon isotope mass balance model, although the contribution of tectonic forcing to the carbon cycle system is not

included in both models.

In this respect, the result of the variations of F_B^C obtained here is not equivalent to the result of either the simple carbon isotope model or the full carbon cycle model, but is similar to the result of a system analysis of the full carbon cycle model which only considers variations of the biological forcing [*Tajika*, 1998, 1999].

3.3. Chemical Weathering and Climate Change

Figure 4 shows variations of chemical weathering rate normalized to the present rate (= f_B x f_E) for the Cases I and II. Note that the Case III (the simple carbon isotope model) assumes it to be constant (= 1). The weathering rate is generally low (especially before the glaciations), but increases rapidly after the glaciations, as well as the variations of the carbonate precipitation rate. Because the weathering rate responds to climate change, this indicates that the climate is cool between the glaciations (especially before the glaciations) but becomes warm temporarily after the glaciations. It is noted that, although the variations of the weathering rate can be interpreted as the effect of climate change, the variations obtained here should only represent the effects of the biological forcing, and do not include effects of the tectonic forcing, as mentioned in the previous section.

Figure 5 shows variations of pCO_2 and T_S. These results are obtained from numerical iteration which estimates the factor f_B so that the value estimated from the carbon isotope model may be consistent with the value estimated from the climate model (integration of the factor $f_B(T, pCO_2)$ from the pole to the equator). Then, the globally-averaged surface temperature is obtained from averaging the surface temperatures from the pole to the equator.

As expected from the results of weathering rate, pCO_2 and T_S are low before the glaciations, but become high after the glaciations, consistent with the view from the carbon isotope data [e.g., *Kaufman et al.*, 1997; *Hoffman et al.*, 1998a, 1998b]. The pCO_2 and T_S are, however, too high to initiate glaciations (Figure 5): T_S varies between 20°C and 30°C throughout the Neoproterozoic in these cases. This is essentially because we assumed present values of F_D and F_W^O for the standard case, and also because we assumed small value of f_E (= 0.15) during the Neoproterozoic. Because the estimate of F_B^C should be affected by F_D and F_W^O through the carbon isotope mass balance model, F_B^C cannot be small as far as the present values of F_D and F_W^O are assumed (i.e., F_W^C ~ F_W^{C*} = 20 x 10^{12} mol/year; Figure 3b). According to the equation (8), F_B^C should balance with F_W^S and F_W^C, so the weathering rate cannot be small whereas the soil biological activity is small (i.e., f_B x f_E ~ 1 with f_E = 0.15). Therefore, f_B, hence pCO_2 and T_S should be high in this case.

These results would, however, change when we assume different values of carbon fluxes in the model. We therefore need parameter studies in order to investigate relationship between the carbon cycle and the climate change.

3.4. Effects of Carbon Fluxes

Figure 6 shows the result of the case for assuming the lower degassing rate (F_D = 1.7 x 10^{12} mol/year). In this case, T_S and pCO_2 become low enough to initiate global glaciations when F_B^O increases. It is noted that the condition for initiation of global glaciation used here is obtained from the 1D-EBM (see the section 2 and Figure 2), so the condition may be different when one assumes different values of the model parameters or different climate models.

It is, however, important to note here that the increase in the organic carbon burial rate as inferred from the positive excursion of $\delta^{13}C_a$ [e.g., *Kaufman et al.*, 1997; *Hoffman et al.*, 1998b] may not be enough to cause global glaciations, and carbon fluxes other than the organic carbon burial rate may also be important for considering the climate change during the Neoproterozoic. In this case (Figure 6), global glaciations occur four times during the Neoproterozoic because of low F_D in addition to the increases of F_B^O. It is, however, noted that, because the input flux of CO_2 into the atmosphere-ocean system is low, F_B^O increases to the level similar to the present but never becomes larger in this case.

If we assume that the glaciations were caused at the time of the positive excursions of $\delta^{13}C_a$ [e.g., *Kaufman et al.*, 1997; *Hoffman et al.*, 1998b], we can investigate the conditions for the carbon fluxes to cause the climate instability based on the equations (6)-(8) analytically. Figure 7 shows the result: in order to cause the climate instability, the degassing rate of CO_2 via metamorphic/volcanism (F_D) and the oxidative weathering rate of organic carbon (F_W^O) should be in the left side of each line which represents the critical condition for the climate system at a specific peak value of positive excursion of $\delta^{13}C_a$ (e.g., positive peak values during the Neoproterozoic are estimated ranging from 7.5 ‰ [*Hayes et al.*, 1999] to 10 ‰ [*Hoffman et al.*, 1998b]). For example, in order to initiate global glacia-

tion when $\delta^{13}C$ increases to 7.5 ‰, F_D should be < 2 x 10^{12} mol/year (< 1/4 of the present rate) with the present F_W^O value. Similarly, the global glaciation occurs when $\delta^{13}C$ increases to 10 ‰ and F_D is < 4 x 10^{12} mol/year (< 1/2 of the present rate).

The global glaciation also occurs when F_W^O becomes very large (> 15 x 10^{12} mol/year for $\delta^{13}C$ =7.5 ‰, and > 8 x 10^{12} mol/year for $\delta^{13}C$ =10 ‰, with the present F_D value). This is, somewhat, difficult to understand because an increase of F_W^O (which releases CO_2 to the atmosphere-ocean system) results in a decrease of pCO_2 in this case. According to the carbon isotope mass balance model, this may be understood as follows: when F_W^O increases, a large amount of low $\delta^{13}C$ due to organic carbon weathering is delivered to the ocean, but it should be removed from the atmosphere-ocean system by deposition of a large amount of organic carbon, because, actually, $\delta^{13}C_a$ did not decreased but increased to 7.5-10 ‰ at that time. In that case, F_B^C should be low (see the equations (3)-(5) with very small $\delta^{13}C_r$), so F_W^C and F_W^S, hence T and pCO_2 should also be low. When the Earth becomes glaciated, sea level falls owing to the growth of ice sheet, resulting in shallow seafloor sediments exposed. Then, F_B^O may increase at the last stage of cooling. In fact, this might be important for the negative excursion of $\delta^{13}C$ as seen just before the glaciation (see the next section). However, in that case, the carbonate weathering rate may also increase at the same time. Furthermore, it may be difficult to consider F_W^O to have increased to > 2-4 times the present rate during the Neoproterozoic when pO_2 was much lower than it is today. It is therefore more likely that an decrease in F_D would have caused the global glaciations.

3.5. Implication for Snowball Earth

Variation of carbon isotopic composition of seawater during the Neoproterozoic implies repetition of cooling and warming. It is, however, difficult to determine the cause for the global glaciations only from the carbon isotope data. This is because we do not know variations of tectonic forcing (such as volcanic activity) during the Neoproterozoic which also affects the carbon cycle and the climate change. According to the discussion in the previous section, if the global glaciations occurred at the time of the positive excursions of $\delta^{13}C_a$, the increases in F_B^O is not enough to initiate the global glaciations, and the decrease in F_D (probably because of decrease in volcanic activity) is required at the same time. However, the Sturtian glaciation may have occurred at about 750 Ma after the breakup of supercontinent Rodinia [e.g., *Hoffman et al.*, 1998b]. Fragmentation of Rodinia could have provided large area of continental margins at which organic carbon buries effectively, which may have resulted in the CO_2 drawdown [e.g., *Hoffman et al*., 1998b]. In that case, seafloor spreading might have become active, which seems to be inconsistent with a decrease in volcanic activity.

Degassing rate of CO_2, however, may have been generally low and may not have correlated well with the seafloor spreading rate during the Neoproterozoic. Most of the CO_2 degassing today is owing to subduction volcanism, and is derived from decomposition of subducted carbonate [*Sano and Williams*, 1996]. In other words, the total CO_2 degassing rate depends largely on the amount of carbonate subducted as seafloor sediments. The $CaCO_3$-secreting plankton, such as foraminifera and coccolithophorids, arose during the Late Jurassic, and are deposited largely in deep water, making them more susceptible to subduction and thermal decomposition today. Before that, relative proportions of carbonates deposited on shallow platforms and in the deep sea might have been different from now [e.g., *Opdyke and Wilkinson*, 1988; *Volk*, 1989], indicating that the CO_2 degassing rate might have been generally lower and varied owing to changes in the sedimentary environment for carbonates in addition to variation of seafloor spreading rate.

There is, however, an enigma: the $\delta^{13}C$ value of seawater might have decreased before the younger Neoproterozoic glaciation [e.g., *Hoffman et al.*, 1998b; *Hoffman and Schrag*, 2002; *Schrag et al*., 2002]. If it is not an artifact of some unusual alteration process [*Kennedy et al*., 1998], but is primary and real, then the cause for the global glaciation cannot be explained easily. *Hoffman et al*. [1998b] considered that this is due to cessation of marine biological productivity because of colder conditions. There is another interpretation which attributes the negative excursion of $\delta^{13}C$ to release of methane owing to dissociation of seafloor methane hydrate [*Schrag et al*., 2002]. Because accumulation of ^{13}C-depleted carbon from volcanic gas, organic carbon, or methane hydrate may result in an increase of pCO_2, it seems to be difficult to explain the global glaciation. However, *Schrag et al*. [2002] considered that pCO_2 should have decreased considerably owing to accumulation of methane (which is a strong greenhouse gas and could maintain the warm climate) because pCO_2 is controlled through the carbonate-silicate geochemical cycle over millions of years [*Walker et a*l., 1981]. When the release of methane ceased, all the methane is converted to CO_2, but pCO_2

would have been too low to maintain the warm climate, resulting in the global glaciation. Hence methane release might explain not only the negative excursion of $\delta^{13}C$ just before the glaciation but also the cause for the global glaciation [*Schrag et al.*, 2002]. Although this hypothesis may be fascinating, it requires continuous release of methane from hydrates over $>10^5$ years (i.e., it should not be a single event nor several discrete events) and very long residence time of methane in the atmosphere (more than 1000 years compared with less than 10 years today).

The negative excursion might be explained by suppression of marine biological productivity in a stagnant equatorial surface ocean during the climate instability, or by an increase in the organic carbon weathering (see the previous section) or dissociation of methane hydrate at the last stage of cooling with an increase in marine biological productivity (this is required in order to remove an extra light carbon isotope from the surface water). In these cases, the negative excursion may reflect the drop in $\delta^{13}C$ of the surface water, and the timescale should be rather short ($< 10^4$ years). Unfortunately, because the detailed timescale for the negative excursion before the glaciation has not been certain so far, it may still be a matter of debate.

4. CONCLUSION

The carbon cycle and the climate change during the Neoproterozoic are estimated from the improved carbon isotope mass balance model combined with the 1-D EBM and from the $\delta^{13}C$ data. In general, the organic carbon burial rate (F_B^O) is high and the carbonate precipitation rate (F_B^C) is low during the Neoproterozoic. However, F_B^O increases and F_B^C decreases before the glaciations, and F_B^O decreases and F_B^C increases after the glaciations. Because F_B^C should be equal to the cation supply rate due to chemical weathering, the weathering rates, hence T and pCO_2 are also generally low, but decrease before the glaciations and increase after the glaciations. However, when present values of the CO_2 degassing rate (F_D) and the weathering rate of organic carbon are assumed in the model, the climate is too warm to initiate glaciations. In order to cause global glaciations, F_D should be low ($<$ 1/4-1/2 times the present rate) at the time of the positive excursions of $\delta^{13}C$.

Acknowledgments. I would like to thank two anonymous reviewers for their helpful comments. This research was partially supported by Grant-in-Aid for Scientific Research (No.12640419 and No.14403004) of the Japan Society of Promotion of Science.

REFERENCES

Berner, R. A., A model for atmospheric CO_2 over Phanerozoic time, *Am. J. Sci*., 291, 339-376, 1991.

Berner, R. A., GEOCARB II: A revised model of atmospheric CO_2 over Phanerozoic time, *Am. J. Sci.*, 294, 56-91, 1994.

Bidigare, R. R., A. Fluegge, K. H. Freeman, K. L. Hanson, J. H. Hayes, D. Hollander, J. P. Jasper, L. L. King, E. A. Laws, J. Milder, F. J. Millero, R. Pancost, B. N. Popp, P. A. Stenberg, and S. G. Wakeham, Consistent fractionation of $\delta^{13}C$ in nature and in the laboratory: Growth-rate effects in some haptophyta algae, *Global Biogeochem. Cycles*, 11, 279-292, 1997.

Caldeira, K., and J. F. Kasting, Susceptibility of the early Earth to irreversible glaciation caused by carbon dioxide clouds, *Nature*, 359, 226-228, 1992.

Crowell, J. C., *Pre-Mesozoic Ice Ages*: *Their Bearing on Understanding the Climate System*, Geological Society of America Memoir 192, p106, Geological Society of America, 1999.

Drever, J. I., and J. Zobrist, Chemical weathering of silicate rocks as a function of elevation in the southern Swiss alps, *Geochim. Cosmochim. Acta*, 56, 3209-3216, 1992.

Evans, D. A., Stratigraphic, geochronological, and paleomagnetic constraints upon the Neoproterozoic climatic paradox, *Am. J. Sci.*, 300, 374-433, 2000.

Hambrey, M. J., and W. B. Harland, *Earth's Pre-Pleistocene Glacial Record*, Cambridge University Press, Cambridge, 1981.

Hayes, J. M., H. Strauss, and A. J. Kaufman, The abundance of $\delta^{13}C$ in marine organic matter and isotopic fractionation in the global biogeochemical cycle of carbon during the past 800 Ma, *Chemical Geology*, 161, 103-125, 1999.

Hoffman, P. F., and D. P. Schrag, The snowball Earth hypothesis: testing the limits of global change, *Tera Nova*, 14, 129-155, 2002.

Hoffman, P. F., A. J. Kaufman, and G. P. Halverson, Comings and goings of global glaciations on a Neoproterozoic tropical platform in Namibia, *GSA Today*, 8(5), 1-9, 1998a.

Hoffman, P. F., A. J. Kaufman, G. P. Halverson, and D. P. Schrag, A Neoproterozoic Snowball Earth, *Science*, 281, 1342-1346, 1998b.

Hyde, W. T., T. J. Crowley, S. K. Baum, and W. R. Peltier, Neoproterozoic 'snowball Earth' simulations with a coupled climate/ice-sheet model, *Nature*, 405, 425-429, 2000.

Ikeda, T., and E. Tajika, A study of the energy balance climate model with CO_2-dependent outgoing radiation: implication for the glaciation during the Cenozoic, *Geophys. Res. Lett.*, 26, 349-352, 1999.

Jenkins, G. S., Global climate model high-obliquity solutions to the ancient climate puzzles of the Faint-Young Sun Paradox and low-altitude Proterozoic Glaciation, *J. Geophys. Res.*, 105, 7357-7370, 2000.

Jenkins, G. S., and S. R. Smith, GCM simulations of Snowball Earth conditions during the late Proterozoic, *Geophys. Res. Lett*, 26, 2263-2266, 1999.

Kaufman, A. J., A. H. Knoll, and G. M. Narbonne, Isotopes, ice ages, and terminal Proterozoic earth history, *Proc. Nat. Acad. Sci.*, 94, 6600-6605, 1997.

Kennedy, M. J., Runnegar, B., Prave, A. R., Hoffman, K.-H., and Arthur, M. A., Two or four Neoproterozoic glaciations? *Geology*, 26, 1059-1063, 1998.

Kirschvink, J. L., Late Proterozoic low-latitude global glaciation: the Snowball Earth, *in The Proterozoic Biosphere*, edited by J. W. Schopf and C. Klein, pp. 51-52, Cambridge Univ. Press,1992.

Kirschvink, J. L., When all of the oceans were frozen (in French), *La Recherche*, 355, 26-30, 2002.

Kirschvink, J. L., E. J. Gaidos, L. E. Bertani, N. J. Beukes, J. Gutzmer, L. N. Maepa, and R. E. Steinberger, Paleoproterozoic snowball Earth: Extreme climatic and geochemical global change and its biological consequences, *Proc. Nat. Sci. Acad.*, 97, 1400-1405, 2000.

Kump, L. R. and M. A. Arthur, Interpreting carbon-isotope excursions: carbonates and organic matter, *Chemical Geology*, 161, 181-198, 1999.

Lasaga, A. C., J. M. Soler, J. Ganor, T. E. Burch, and K. L. Nagy, Chemical weathering rate law and global geochemical cycles, *Geochim. Cosmochim. Acta*, 58, 2361-2386, 1994.

Opdyke, B. N., and B. H. Wilkinson, Surface area control of shallow cratonic to deep marine carbonate accumulation, *Paleoceanography*, 3, 685-703, 1988.

Poulsen, C. J., R. T. Pierrehumbert, and R. L. Jacob, Impact of ocean dynamics on the simulation of the Neoproterozoic "snowball Earth", *Geophys. Res. Lett.*, 28, 1575-1579, 2001.

Rothman, D. H., J. M. Hayes, and R. E. Summons, Dynamics of the Neoproterozoic carbon cycle, *Proc. Nat. Acad. Sci.*, 199, 8124-8129, 2003.

Sano, Y., and S. N. Williams, Fluxes of mantle and subducted carbon along convergent plate. *Geophys. Res. Lett.*, 23, 2749-2752, 1996.

Schrag, D. P., R. A. Berner, P. F. Hoffman, and G. P. Halverson, On the initiation of a snowball *Earth, Geochem. Geophys. Geosyst.*, 3(6), 10.1029/2001GC000219, 2002.

Schwartzman, D. W., and T. Volk, Biotic enhancement of weathering and the habitability of Earth, *Nature*, 340, 457-460, 1989.

Schwartzman, D. W., and T. Volk, Biotic enhancement of weathering and surface temperatures on earth since the origin of life. *Paleogeogr. Paleoclim. Paleoeco*. (Global and Planetary Change Section), 90, 357-371, 1991.

Schidlowski M., A 3,800-billion-year isotopic record of life from carbon in sedimentary rocks, *Nature*, 333, 313-318, 1988.

Tajika, E., Climate change during the last 150 million years: Reconstruction from a carbon cycle model, *Earth Planet. Sci. Lett.*, 160, 695-707, 1998.

Tajika, E., Carbon cycle and climate change during the Cretaceous inferred from a carbon biogeochemical cycle model, *The Island Arc*, 8, 293-303, 1999.

Tajika, E., Faint young Sun and the carbon cycle: Implication for the Proterozoic global glaciations, *Earth Planet. Sci. Lett.*, 214 (3-4), 443-453, 2003.

Tajika, E., and T. Matsui, The evolution of the terrestrial environment, *in Origin of the Earth*, edited by H. E. Newsom, J. H. Jones, pp. 347-370, Oxford Univ. Press, New York, N.Y., 1990.

Tajika, E., and T. Matsui, Evolution of terrestrial proto- CO_2-atmosphere coupled with thermal history of the Earth, *Earth Planet. Sci. Lett.*, 113, 251-266, 1992.

Volk, T., Sensitivity of climate and atmospheric CO_2 to deep-ocean and shallow-ocean carbonate burial, *Nature*, 337, 637-640, 1989.

Walker, J. C. G., P. B. Hayes, and J. F. Kasting, A negative feedback mechanism for the long-term stabilization of Earth's surface temperature, *J. Geophys. Res.*, 86, 9776-9782, 1981.

Williams, G. E., History of the Earth's obliquity, *Earth Sci. Rev.*, 34, 1-45, 1993.

E. Tajika, Department of Earth and Planetary Science, Graduate School of Science, University of Tokyo, 7-3-1 Hongo, Bunkyo-ku, Tokyo 113-0033, Japan. (e-mail: tajika@eps.s.u-tokyo.ac.jp)

FIGURE CAPTIONS

Figure 1. Variations of carbon isotopic composition of sea-water (data from *Hayes et al*. [1999]). Positive and negative excursions of $\delta^{13}C$ may correlate with glaciations (represented by triangles) [e.g., *Kaufman et al*., 1997; *Hoffman et al*., 1998a] during the Neoproterozoic.

Figure 2. (a) Variation of latitudinal distribution of surface temperature due to decrease in pCO_2. The results obtained from the 1-D EBM with standard parameters' values (ice albedo = 0.62 and land/ocean albedo = 0.3, and diffusion coefficient for latitudinal heat transport of 0.455 $Wm^{-2} K^{-1}$). (b) Variation of silicate weathering rate (normalized to the present rate of 6.65 x 10^{12} mol/year [*Berner*, 1994]) due to decrease in pCO_2 (PAL= present atmospheric level). Solid lines represent stable solutions (ice-free and partially ice-covered), and dotted lines represent unstable solutions. The effective solar constant S_{eff} is 1 at present and 0.94 for the Neoproterozoic.

Figure 3. Variations of (a) organic carbon burial rate and (b) carbonate precipitation rate during the Neoproterozoic. Solid curves represent the Case I (high resolution $\delta^{13}C_a$ data set by *Hayes et al*. [1999] with the formulation of Δ by *Kump and Arthur* [1999]). Dashed curves represent the Case II (low resolution $\delta^{13}C_a$ and $\delta^{13}C_g$ data sets by *Hayes et al*. [1999]). Dotted curves represent the Case III (the simple carbon isotope mass balance model with low resolution $\delta^{13}C_a$ and $\delta^{13}C_g$ data sets by *Hayes et al*. [1999]).

Figure 4. Variations of chemical weathering rate normalized to the present rate (= f_B x f_E) during the Neoproterozoic for the Cases I (solid curves), II (dashed curves), and III (dotted curves).

Figure 5. Variations of (a) CO_2 level (in PAL) and (b) globally-averaged surface temperature during the Neoproterozoic for the Cases I (solid curves) and II (dashed curves).

Figure 6. Variations of the globally-averaged surface temperature during the Neoproterozoic for the case of low CO_2 degassing rate (= 1.7 x 10^{12} mol/year, < 1/4 of the present rate) with high resolution $\delta^{13}C_a$ data set by *Hayes et al*. [1999] and the formulation of Δ by *Kump and Arthur* [1999].

Figure 7. Conditions of the carbon fluxes required for causing global glaciation at the positive excursion of $\delta^{13}C$. Each figure represents the peak value of the positive excursion (in ‰). Global glaciation may be caused when the CO_2 flux conditions are in the left side of each line. These results are obtained from solving the equations (6)-(8) analytically (Δ is assumed here to be 25 ‰) and from the standard result of the 1-D EBM.

Figure 1 (Tajika)

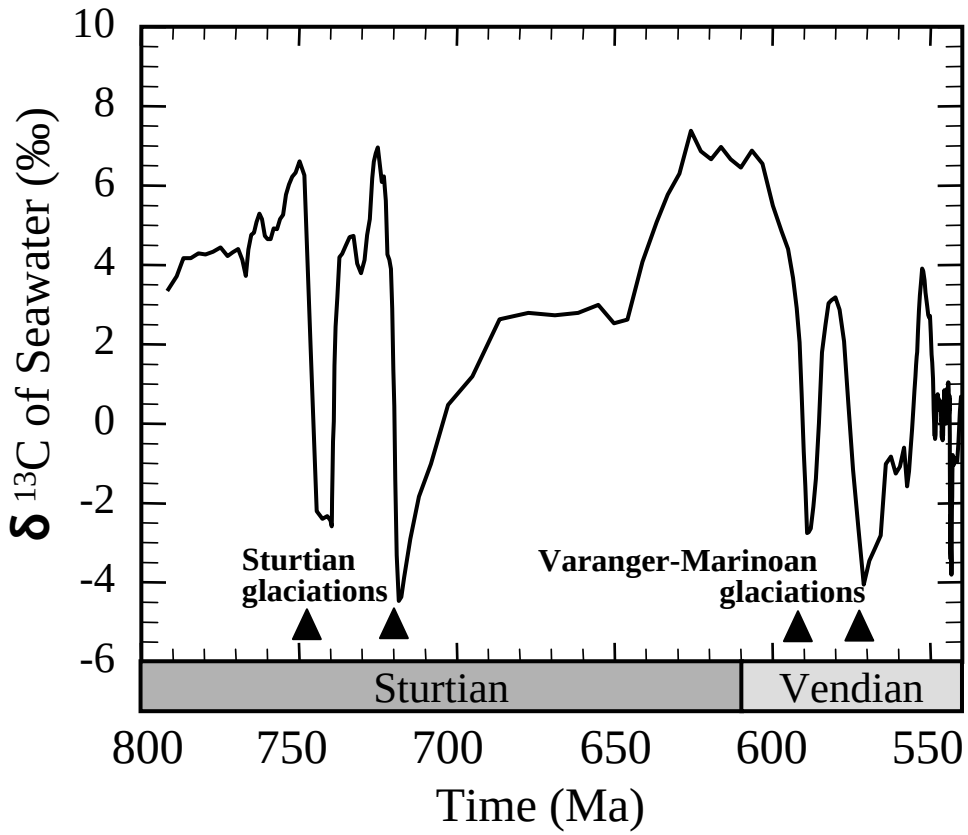

Figure 2 (Tajika)

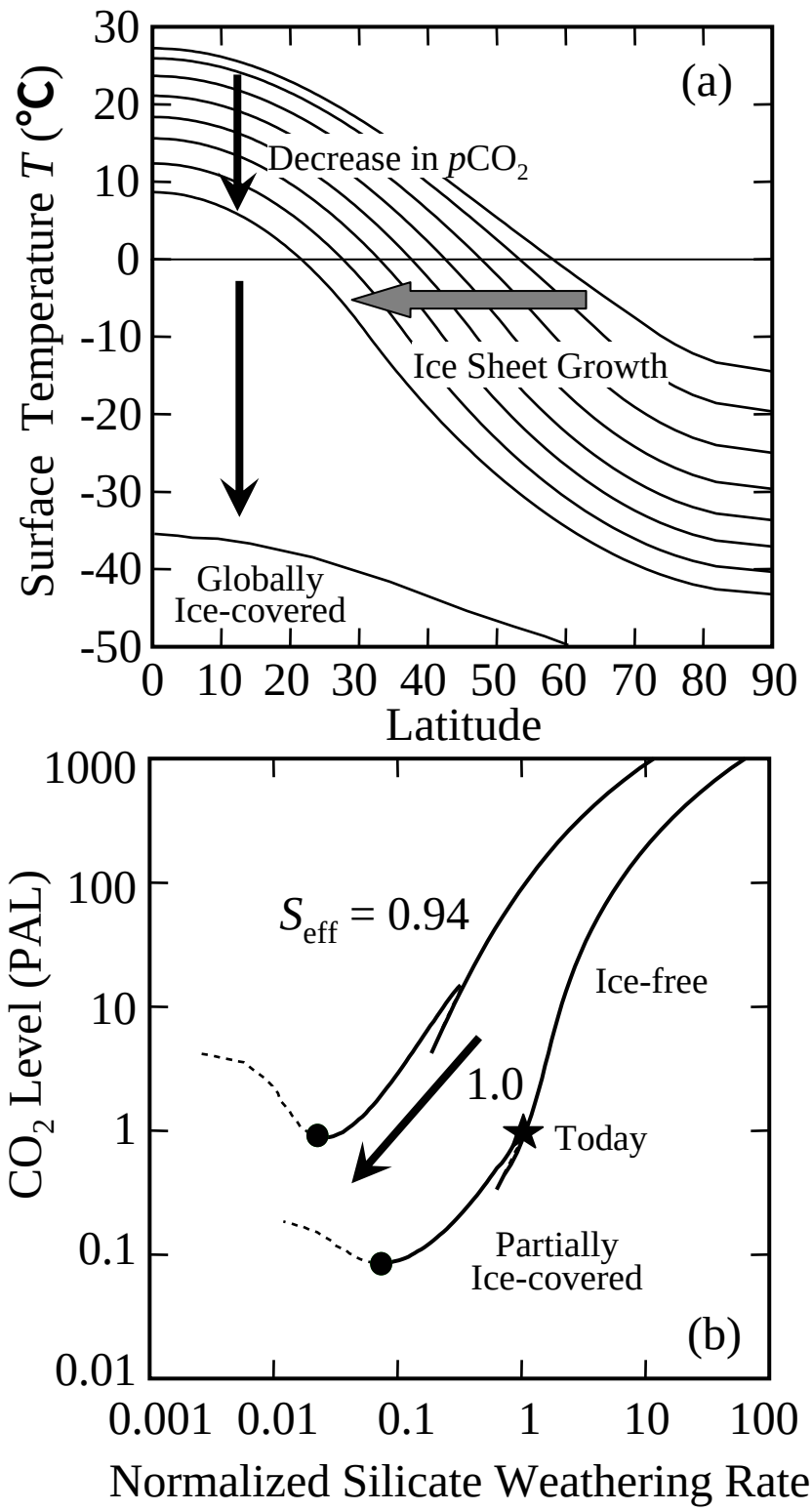

Figure 3 (Tajika)

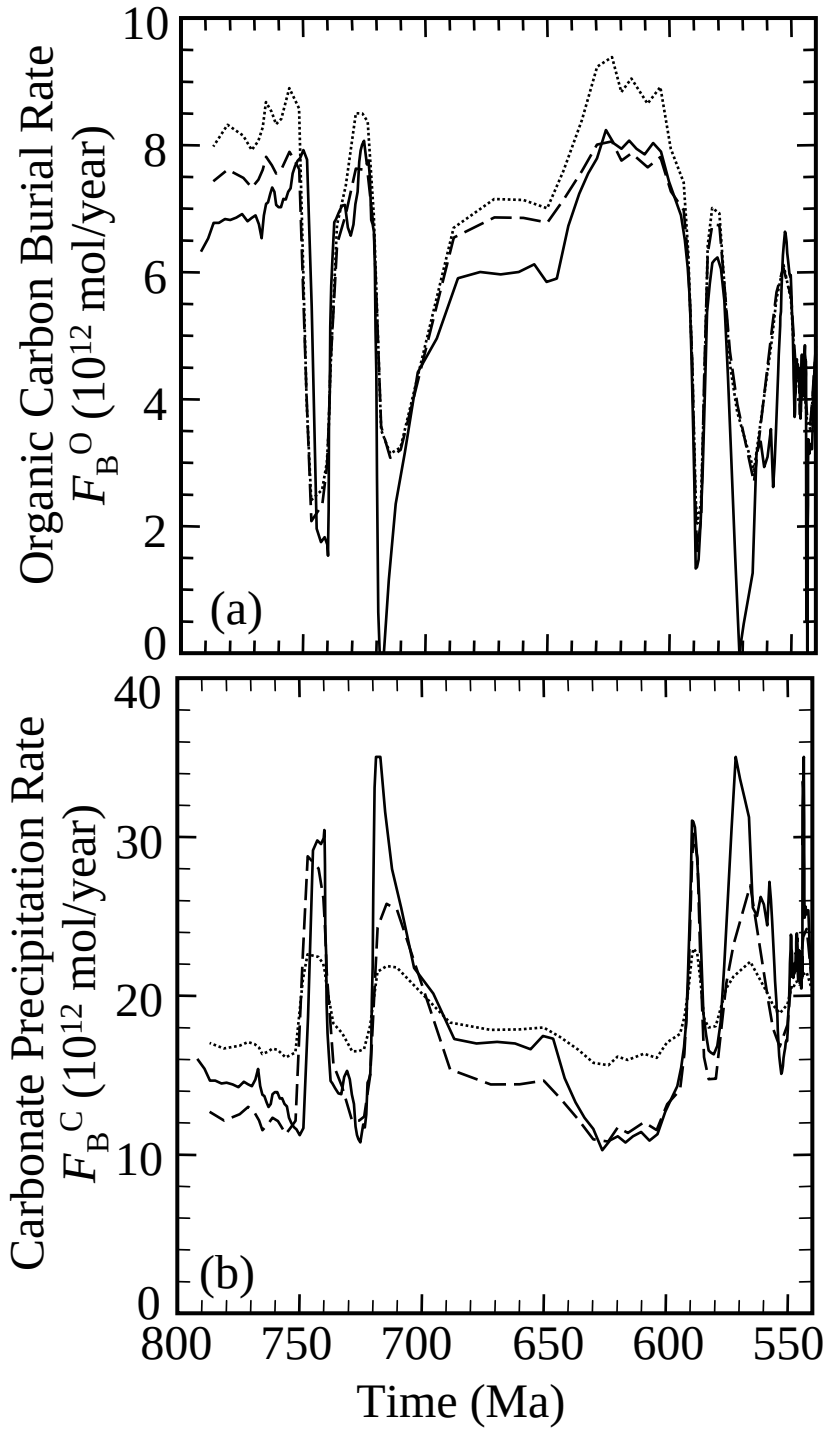

Figure 4 (Tajika)

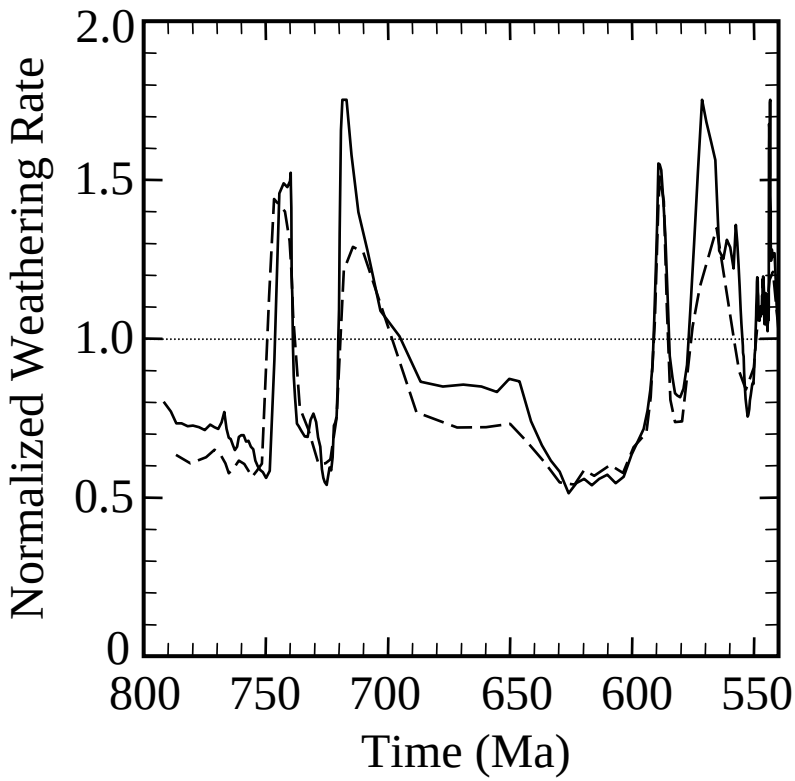

Figure 5 (Tajika)

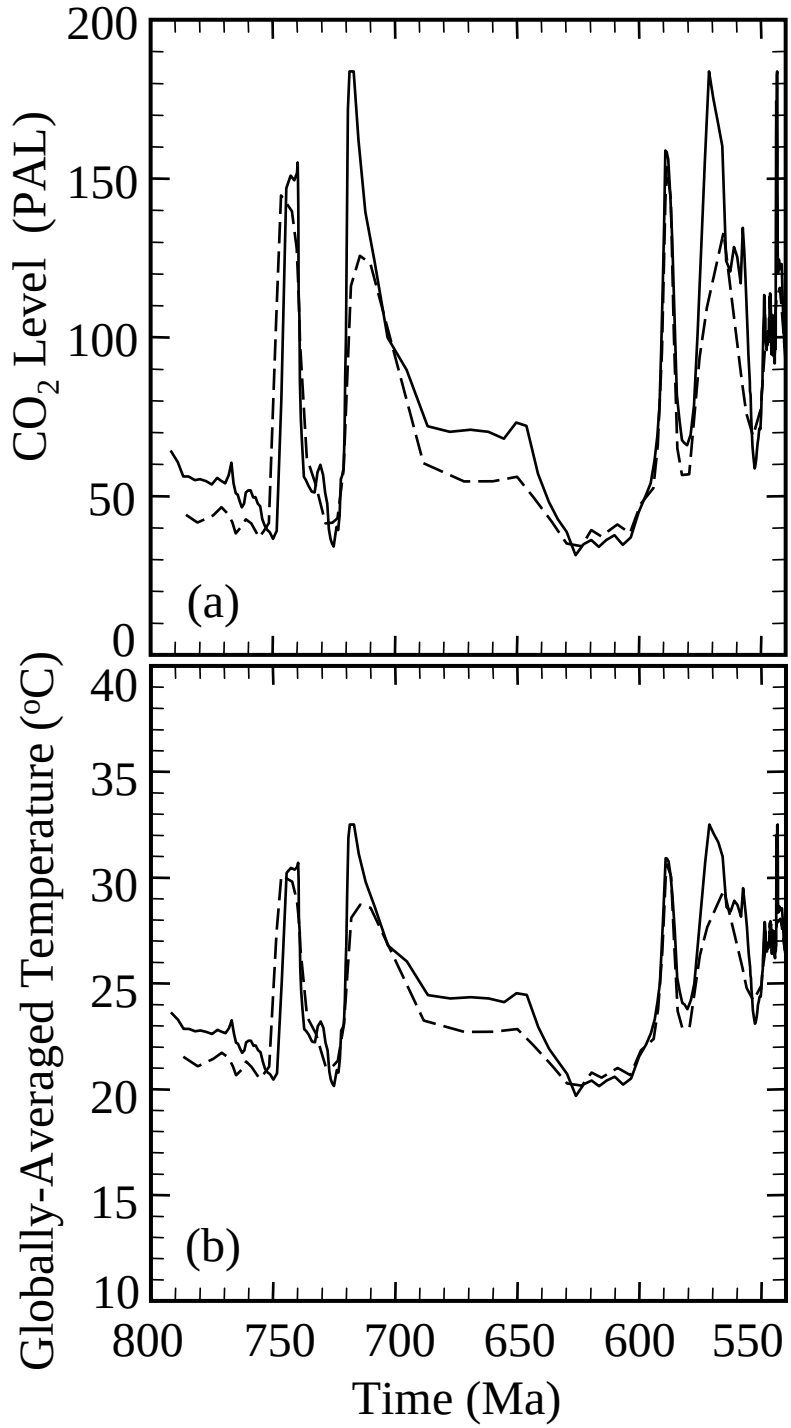

Figure 6 (Tajika)

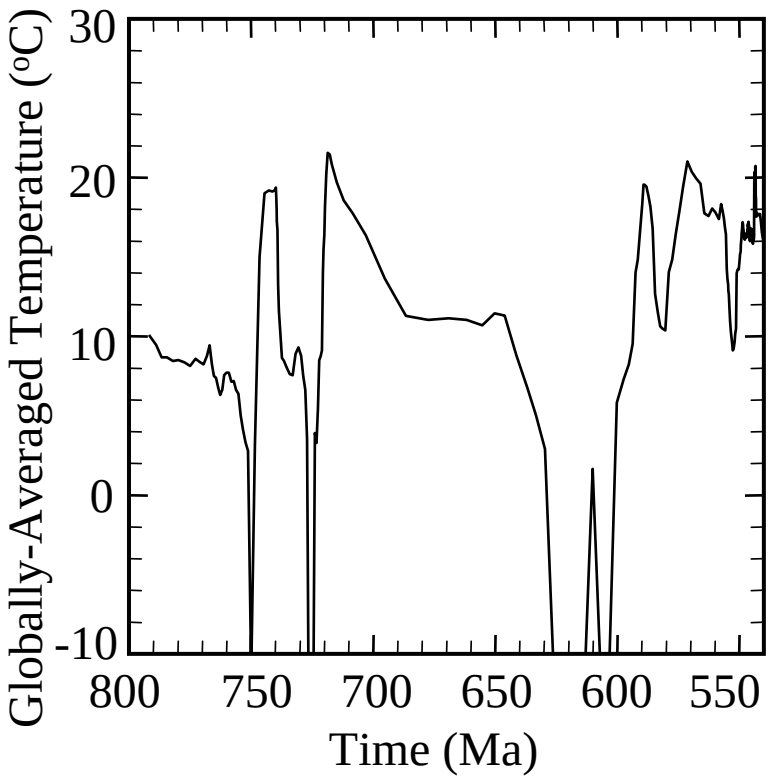

Figure 7 (Tajika)